Resilient Poly(α-Hydroxy Acids) with Improved Strength and Ductility via Scalable Stereosequence-Controlled Polymerization

Xiaoqian Wang,[1] Ai Lin Chin,[1] Jingyi Zhou,[2] Hua Wang,[2] and Rong Tong[1,*]

[1] Department of Chemical Engineering, Virginia Polytechnic Institute and State University, 635 Prices Fork Road, Blacksburg, Virginia, 24061, United States.

[2] Department of Materials Science and Engineering, University of Illinois, 1304 West Green Street, Urbana, Illinois, 60801, United States

ABSTRACT: Despite the degradability and biocompatibility of poly(α-hydroxy acids), their utility remains limited because their thermal and mechanical properties are inferior to those of commodity polyolefins, which can be attributed to the lack of side-chain functionality on the polyester backbone. Attempts to synthesize high-molecular-weight functionalized poly(α-hydroxy acids) from *O*-carboxyanhydrides have been hampered by scalability problems arising from the need for an external energy source such as light or electricity. Herein, we report an operationally simple, scalable method for the synthesis of stereoregular, high-molecular-weight (>200 kDa) functionalized poly(α-hydroxy acids) by means of controlled ring-opening polymerization of *O*-carboxyanhydrides mediated by a highly redox reactive manganese complex and a zinc-alkoxide. Mechanistic studies indicated that the ring-opening process likely proceeded via the Mn-mediated decarboxylation with alkoxy radical formation. Gradient copolymers produced directly by this method from mixtures of two *O*-carboxyanhydrides exhibited better ductility and toughness than their corresponding homopolymers and block copolymers, therefore highlighting the potential feasibility of functionalized poly(α-hydroxy acids) as ductile and resilient polymeric materials.

INTRODUCTION

The past 100 years have witnessed tremendous progress in polymer science, and the widespread need of polymeric products has worldwide production of commercial plastics exceeding 350 million tons in 2019. Regrettably, excessive disposal of nondegradable plastic waste in landfills causes severe environmental consequences because the accumulated waste can persist in ecosystems for hundreds of years.[1] Therefore, considerable research effort has been devoted to the search for degradable substitutes to be transformed into commodity thermoplastics as single-use materials.[2] Among the degradable polymers developed on the basis of this research, aliphatic polyesters have shown exceptional promise because they are made from renewable resources, and their chemical or enzymatic degradation products are environmentally benign and can be recycled.[2b,3] In particular, stereoregular[4] and stereosequence-controlled polyesters[5] synthesized by metal-catalyzed stereoselective ring-opening polymerization (ROP) of racemic monomers show enhanced physical and mechanical properties relative to their atactic counterparts.[6]

Nevertheless, the practical utility of the commercially available polyesters, including poly(α-hydroxy acids), is limited because their thermal and mechanical properties are inferior to those of commodity polyolefins. For example, poly(lactic acid) (PLA) and poly(3-hydroxybutyrate) are brittle and lack toughness (< 5% elongation at break).[7] Additionally, the upper-use temperatures of many aliphatic polyesters are restricted because of their moderate or low glass-transition temperatures (T_g): PLA ($T_g \approx 45$ °C), poly(3-hydroxybutyrate) ($T_g \approx 5$ °C), and polycaprolactone ($T_g \approx -60$ °C). These limitations can be attributed to the lack of functional groups on the aliphatic polyester backbone. Indeed, the incorporation of functional groups on the backbone of polyolefins can alter their processability, adhesion, miscibility, and mechanical strength (Figure 1a).[8] However, the incorporation of pendant functional groups onto lactones, which are the monomers used for ROP to generate polyesters, is challenging in that it usually requires multistep syntheses that are difficult to scale up.[9] In addition, alternative monomers, such as 1,3-dioxolan-4-one, fail to produce high-molecular-weight (MW) polymers (< 20 kDa) because of side reactions (Figure 1b).[10]

In the quest for practicality, *O*-carboxyanhydrides (OCAs)—which are prepared from amino or hydroxy acids—are perhaps the most ubiquitous class of highly active monomers with pendant functional groups used for ROP to afford functionalized polyesters.[11] However, the ROP of these monomers presents certain challenges. Notably, organocatalysts typically used for the ROP of OCAs exhibit low activity for the synthesis of high-MW polymers, and these catalysts cannot mediate stereoselective ROP of OCAs to form polyesters with various tacticities (Figure 1c). To overcome such challenges, we have recently demonstrated that the combination of light or electricity with organometallic catalysts produces stereoregular, high-MW polyesters (> 200 kDa) with various microstructures (Figure 1c).[5b,12] Despite the efficiency of these reactions, their reliance on an external energy source makes them impractical for large-scale synthesis of high-MW polymers, including stereosequence-controlled copolymers.

Herein, we report a new method for achieving rapid and controlled OCA polymerization using highly reactive metal complexes without the need for an external energy source, and we describe the use of this method for large-scale preparation of stereoregular polyesters and stereosequence-controlled copolymers bearing various

pendant functional groups on a large scale (Figure 1d). The synthesized polyesters are amenable to quantitative chemical recycling under mild conditions. Gradient copolymers synthesized by means of this method exhibit enhanced ductility and toughness compared to those of homopolymers and block copolymers synthesized from the same OCA monomers.

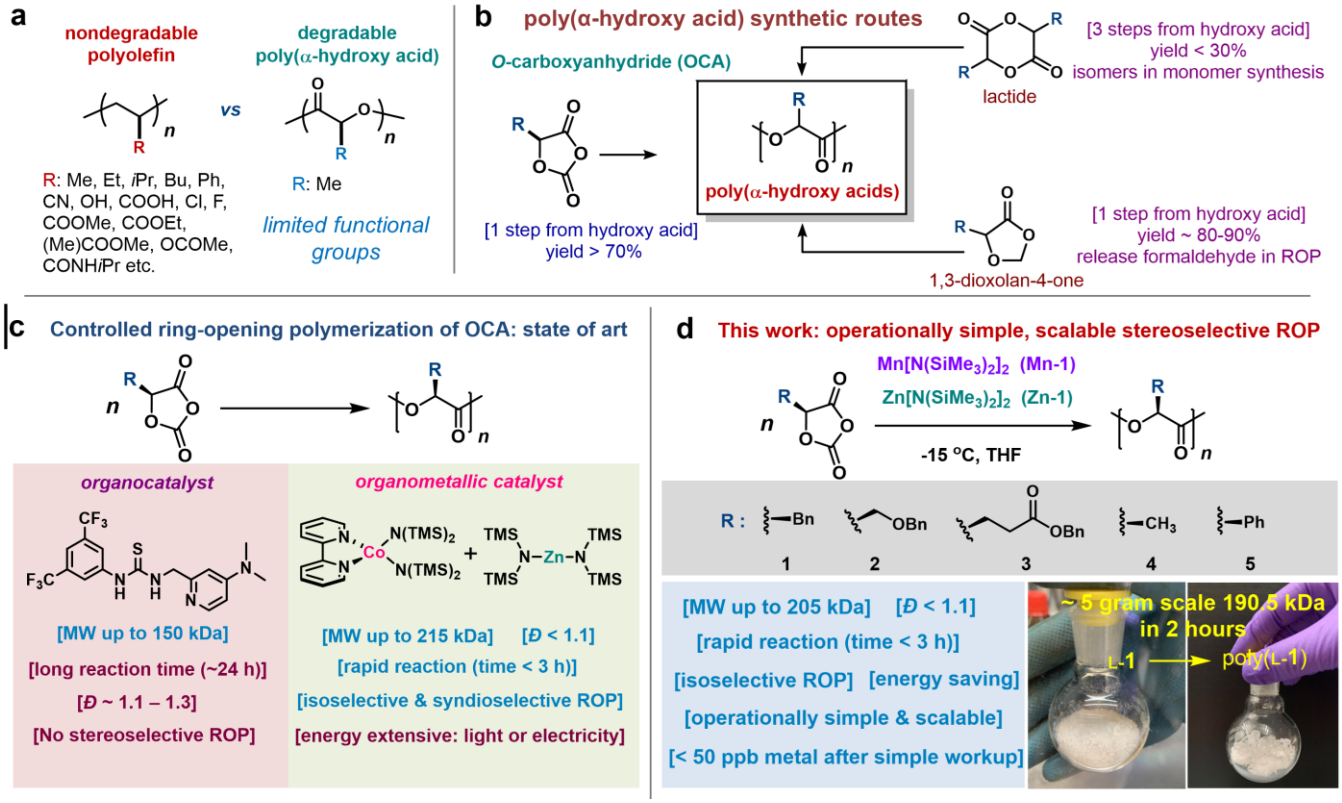

Figure 1. Scalable ring-opening polymerization (ROP) of *O*-carboxyanhydrides (OCAs). (a) Functionalized nondegradable polyolefins and degradable poly(α-hydroxy acids), which have a limited variety of pendant functional groups. (b) Synthetic routes to poly(α-hydroxy acids). (c) Previously reported uses of organocatalysts and organometallic catalysts for ROP of OCAs, with pros and cons indicated in blue and red type, respectively. (d) Scalable stereoselective ROP of OCAs reported in this paper to prepare stereosequence-controlled resilient polyesters with enhanced strength and ductility.

RESULTS AND DISCUSSION

Mechanism-driven identification of Mn/Zn complexes for controlled ROP of OCAs. Currently, no single metal complex or organocatalyst can efficiently mediate controlled ROP of OCAs to prepare high MW polymers (over 100 kDa) with controls over stereoselectivity and stereosequence. In prior studies, we showed that at least two metal complexes are needed to prepare high-MW (>100 kDa) polyesters by ROP of OCAs: (i) a metal-alkoxide (e.g., Zn-alkoxide) for chain propagation and (ii) a metal complex (Ni/Ir or Co) activated by external energy for OCA decarboxylation, a key step that allowed the metal-alkoxide to engage with OCA and prevented the formation of inactive metal-carbonate complexes (Figure 2a).[11b,12b] The use of external stimuli such as light and electricity greatly challenges the scalability of the synthetic process for mass production for further advances in the field of degradable polyesters. To overcome such problems, we hypothesized that a redox-active transition-metal complex could be combined with a Zn-alkoxide catalyst to mediate controlled ROP without the assistance of an external energy source (light or electricity). Recent advances in organometallic chemistry,[13] as well as the wide range of known metalloenzyme-mediated redox reactions,[14] inspired us to attempt to identify a suitable redox-active transition-metal complex. In particular, we explored earth-abundant transition metals because they are less expensive than rare-earth metals and they readily undergo oxidation state changes—that is, lose or gain electrons—to mediate chemical reactions.[15] We set about investigating stable low-coordination-number metal (trimethylsilyl)amide complexes (Co, Mn, Fe, Ce, and Y) because these well-characterized redox-active complexes can be easily synthesized in one step on a large scale (Figure 2b).[16] Note that none of them has been utilized for decarboxylation without external energy activation.

To test our hypothesis, we performed ROP of L-PheOCA (L-**1**) using various metal silylamide complexes in the presence of Zn(HMDS)$_2$ (**Zn-1**; HMDS, hexamethyldisilazane) and BnOH ([L-**1**]/[M]/[**Zn-1**]/[BnOH] = 500/1/1/1; Figure 2b). We evaluated the performance of the complexes in terms of monomer conversion and the number-average MWs and MW distributions (M_n, and $Đ$, respectively) of the resulting polymers (Figure 2b) and found that the optimal combination consisted of **Zn-1** and Mn(HMDS)$_2$ (**Mn-1**, Tables S1 and S2). Monomer conversion

was completed within 1 hour at −15 °C, and poly(L-**1**) with a M_n of 83.5 kDa and a $Đ$ of 1.08 was obtained (expected MW, 74.1 kDa). In contrast, the remaining tested metal silylamides either failed to fully polymerize L-**1** or could not control polymer's MW (Figure 2b, Tables S1 and S2). Among the examined complexes, the Mn^{II} complex seemed to have the ideal balance of metal electronegativity and metal–nitrogen bond length (Figure 2b). This result is consistent with the fact that the Mn center of some enzymes, including oxalate decarboxylase, can mediate radical decarboxylation reactions.[17] To the best of our knowledge, there are no reports on using metal silylamides for decarboxylation without external energy activation. Therefore, this unique strategy provides a new entry to scale up poly(α-hydroxy acids) with pendant functional groups.

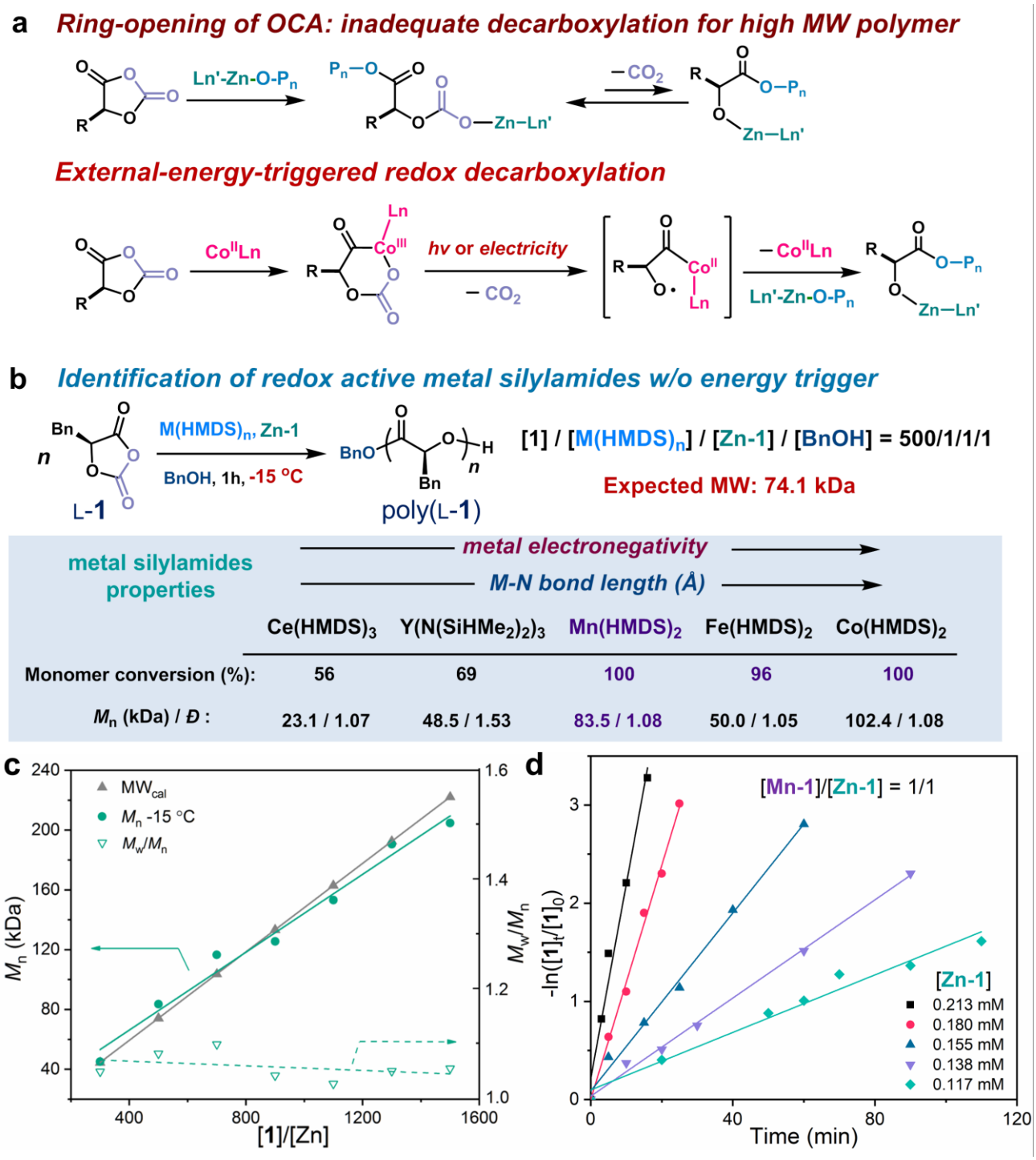

Figure 2. Mechanism-inspired identification of Mn/Zn catalysts for ring-opening polymerization of *O*-carboxyanhydrides (OCAs). (a) Mechanisms of inadequate decarboxylation in Zn-mediated ROP of OCAs, which can be overcome by external-energy-triggered, Co-mediated decarboxylation ring-opening and enchainment of OCAs. (b) Identification of the optimal metal silylamide complex for ring-opening polymerization of OCAs involving redox decarboxylation without an external energy source, on the basis of metal electronegativity and metal–nitrogen bond length.[16b] Expected MW: molecular weight calculated based on the feed ratio assuming 100% monomer conversion. (c) Plots of M_n and MW distribution (M_w/M_n) of poly(L-**1**) versus [L-**1**]/[Zn] ratio at −15 °C ([**Mn-1**]/[**Zn-1**]/[BnOH] = 1/1/1). (d) Plots of L-**1** conversion versus time at various **Zn-1** concentrations. [L-**1**] = 0.150 M; [**Mn-1**]/[**Zn-1**]/[BnOH] = 1/1/1.

By means of a series of control experiments, we demonstrated the necessity for each of the catalytic components (Table 1). Without **Mn-1**, the polymerization was uncontrolled with a monomer conversion of 25.7% (entry 2), whereas **Zn-1** was essential for chain propagation (entry 3). In the absence of the initiator, BnOH, the obtained polymer had uncontrolled M_n and $Đ$ values and a low monomer conversion (entry 4). Electrospray ionization mass spectrometry (ESI-MS) and matrix-assisted laser desorption/ionization (MALDI) analysis of oligo(L-**1**) confirmed the attachment of the BnO- group to the oligomer (Figure S1), suggesting that a Zn-

alkoxide was involved in ring-opening and chain propagation. Irradiation with light had a negligible effect on the MW and $Đ$ values of the polymer (Table 1, entry 7; Figure S2a), indicating that light was not required. Monomer conversion was incomplete when the polymerization was performed at room temperature (entry 8), indicating that the low temperature (−15 °C) prevented side reactions that hindered chain propagation (Figure S2b).[11b,12b] We found that the addition of ligands to **Mn-1** did not markedly improve its polymerization activity (Table S4); and other commercially available Mn complexes were unable to mediate controlled ROP at a high feed ratio (Table S5).

Table 1. Optimization of Conditions of Ring-Opening Polymerization of L-1 [a]

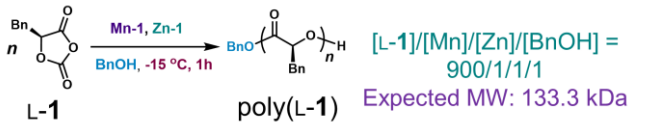

Entry	Condition	Conv. % [b]	M_n (kDa) [c]	MW_{cal} (kDa)	$Đ$ [c]
1	As shown	100	125.5	133.3	1.04
2	No **Mn-1**	25.7	63.6	34.3	1.14
3	No **Zn-1**	7.6	9.17	10.2	1.42
4	No BnOH	21.9	20.2	29.3	1.26
5	Only **Mn-1**	0	-	0	-
6	Only **Zn-1**	26.2	62.1	35.0	1.16
7	Light	100	125.1	133.3	1.04
8	20 °C	21.9	31.3	29.3	1.13

[a] Abbreviations: Conv., monomer conversion; M_n, number-average molecular weight; $Đ$, molecular weight distribution; MW_{cal}, molecular weight calculated based on the feed ratio and monomer conversion; expected MW: molecular weight calculated based on the feed ratio assuming 100% monomer conversion. Polymerization condition: [L-**1**]/[**Zn-1**]/[**Mn-1**]/[BnOH] = 900/1/1/1 at −15 °C in a glove box. [b] Determined from the intensity of the Fourier transform infrared peak at 1805 cm^{-1}, which corresponds to the anhydride group of the *O*-carboxyanhydride. [c] Determined by gel-permeation chromatography.

Using the optimized conditions, we evaluated the effect of the initial [L-**1**]/[Mn]/[Zn] feed ratio on the M_n of the poly(L-**1**) product and found that M_n increased linearly as the feed ratio was increased up to 1500/1/1. At this ratio, the resulting product had a M_n of 204.7 kDa and a $Đ$ of 1.05 (Figure 2c; gel-permeation chromatograms of the polymers are shown in Figure S3). These feed ratio and M_n values are higher than any other reported values for the ROP of OCAs.[11b,12a,18] At all the tested feed ratios, the $Đ$ values of the obtained polymers were less than 1.1, suggesting that chain-breaking reactions did not occur during ROP.[19] No epimerization of the α-methine hydrogen was observed either in the homodecoupled ^{1}H NMR spectrum of a high-MW poly(L-**1**) (Figure S4) or in the spectra of products obtained by ROP of OCA monomers **2**–**5** (see Figure 1d for the structures of **2**–**5**, Table S6 for ROP results, and Figures S5–8 for ^{1}H NMR spectra of polymer products). Although considerable epimerization of L-**5** is often observed during ROP,[20] this was not the case in our system (Figure S8). Additionally, Mn/Zn-mediated ROP of L-**1** at −15 °C exhibited first-order reaction kinetics with a reaction order of 4.60 ± 0.35 at the fixed Mn/Zn ratio of 1/1 (Figure 2d; Figure S2c). We also examined the kinetics of the ROP by varying the concentration of each reaction component (Figure S2d-h), and discovered that the kinetics of the ROP of L-**1** follows an overall kinetic law of the form:

$$-d[\text{L-}\mathbf{1}]/dt = k_p[\mathbf{Mn\text{-}1}]^{2.10}[\mathbf{Zn\text{-}1}]^{2.51}[\text{L-}\mathbf{1}]^{1} \quad (1)$$

where k_p is the rate constant of chain propagation. These results indicated no formation of Mn–Zn complex during the ROP, and the rate of chain propagation was independent of BnOH concentration.

Since the workup for the polymerization process was simple, the synthesis of polymers and copolymers could easily be scaled up to over 3 g (photos in Figure 1d), allowing for the preparation of polymer specimens in sufficient quantities for mechanical testing (*vide infra*). Furthermore, diblock and triblock copolymers could also be readily prepared by sequential addition of the monomers, and remarkable control of the M_n and $Đ$ values was achieved (Table S7, Figures S9–21).

Scheme 1. Efficient degradation of poly(α-hydroxy acids) to α-hydroxy acid, fulfilling the recycling circle.

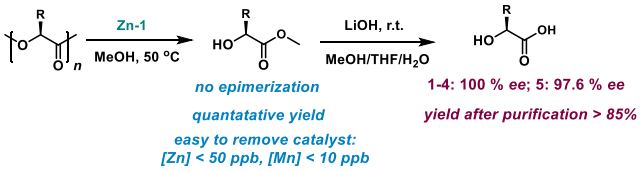

Chemical recycling of functionalized poly(α-hydroxy acids). Many polyesters are amenable to recycling via enzymatic or chemical degradation.[3b,21] Poly(L-**1**) was degraded by treatment with **Zn-1** (10 wt%) in MeOH at 50 °C for 12 h (Scheme 1), which yielded pure methyl ester quantitatively, as indicated by the ^{1}H NMR and ESI-MS spectra of the degradation reaction solution (Figure S22). After the degradation reaction was completed, an insoluble Zn-alkoxide complex was formed in the MeOH solution[21] and could be easily removed by filtration through silica gel, and the enantiopure methyl ester was recovered by evaporation of the filtrate (89.7 % yield, Scheme 1). This method could be extended to OCA monomers **2**–**5**, all of which could be efficiently and completely degraded to their corresponding enantiopure methyl ester forms, measured by chiral HPLC (Figures S23–26; no absorbance from degraded methyl esters of **3** and **4**; HPLC, high-performance liquid chromatography). Using inductively coupled plasma mass spectrometry, we confirmed that negligible amount of Zn remained in the filtrate ([Zn] < 50 ppb, Table S8). The obtained methyl esters are value-added chemicals,[22] and they could be rapidly transformed to hydroxy acids by reacting with LiOH at room temperature within 4 hours (Scheme 1).[23] No epimerization occurred in the obtained hydroxy acids degraded from all polymers synthesized from L-**1** to L-**4** (Figures S22-25), and only slight epimerization occurred for L-**5** (97.6 % *ee*), determined by chiral HPLC (Figure S26). This two-step facile degradation strategy, therefore, closes the recycling loop. Note that polyesters with pendant side-chain groups are difficult to completely degrade using conventional methods (Table 2, Figure S27).[3b,24] Our degradation method is superior to many degradation

methods, which tend to require high temperature, prolonged reaction time, and extra steps for separation of catalysts from depolymerized products,[25] in addition to suffering from side reactions that generate substantial epimerized products.[26]

Table 2. Degradation of poly(L-1) by Zn-1/MeOH benchmarked against conventional methods [a]

Entry	Condition	Solvent	Temp. (°C)	Time (h)	Conv. (%) [b]
1	10 wt% **Zn-1**	MeOH	50	12	100 [d]
2	/	MeOH	50	12	0
3	1 M NaOH [24b]	Water	50	12	9.2 [c]
4	10 wt% $ZnCl_2$	MeOH	50	12	0
5	2 mol% $ZnCl_2$ [3b]	Toluene	120	24	0
6	10 wt% TBD [24a]	MeOH	50	12	86.1

[a] Abbreviation: Temp., temperature; Conv., conversion to methyl ester of **1**; TBD, 1,5,7-triazabicyclo[4.4.0]dec-5-ene. Poly(L-**1**) used for degradation: M_n = 78.4 kDa, $Đ$ = 1.05. [b] Determined by ^{1}H NMR analysis of the reaction solution (Figure S27). [c] Determined by the weight of dried poly(**1**) after the reaction. [d] No epimerization, measured by chiral HPLC (Figure S22).

Mechanistic Studies. We drew upon our knowledge of the mechanisms of photoredox ROP[11b] and electrochemical ROP by Co/Zn[12a] to develop a plausible redox ROP mechanism. The catalytic cycle starts with the oxidative addition of **Mn-1** to the OCA to form the Mn^{IV} species **A** (Scheme 2). Unlike the Co complex used in our electrochemical ROP,[12a] which exhibits only one reversible redox wave in cyclic voltammetry measurements ($E_{1/2}^{red}[Co^{III}/Co^{II}]$ = 0.77 V vs SCE [saturated calomel electrode], where $E_{1/2}^{red}$ is the redox half-wave potential),[12a] **Mn-1** exhibited two quasi-reversible redox waves: $E_{1/2}^{red}[Mn^{III}/Mn^{II}]$ = 0.60 V and $E_{1/2}^{red}[Mn^{IV}/Mn^{III}]$ = 1.15 V versus SCE (Figure S28a). The formation of Mn^{IV} species **A** (Scheme 2) was supported by the observation that the $E_{1/2}^{red}[Mn^{III}/Mn^{II}]$ peak had disappeared almost completely within 5 min after the start of the ROP of a L-**1**/**Mn-1**/**Zn-1**/BnOH (1000/1/1/1) mixture at −15 °C, whereas the $E_{1/2}^{red}[Mn^{IV}/Mn^{III}]$ peak (1.22 V) persisted throughout the ROP (Figure S28b). Given that the oxidation potential of amino acid carboxylates (e.g., $E_{1/2}^{red}$ = 0.83 V versus SCE for *N*-(carbobenzyloxy)-L-phenylalanine) and literature reports,[13,27] the single-electron transfer (Mn^{IV}/Mn^{III}) process is likely to be thermodynamically favored over the two-electron transfer process (Mn^{IV}/Mn^{II}).[28]

We further investigated the ring-opening process by analyzing the reaction of an L-**1**/**Mn-1**/**Zn-1**/BnOH (1/1/1/1) mixture at −15 °C via ESI-MS (Figure 3a), which revealed the presence of BnO-terminated oligomers **G1** and **G2**, thus confirming the necessity of Zn-alkoxide for chain propagation (note that the Mn complex are paramagnetic and attempts to study the reaction by NMR were not successful). Moreover, detection of intermediate **H** and its carbonyl complexes **I1**–**I3**[29] in the mass spectrum (Figure 3a, Figure S29) indicated that **Mn-1** inserts regioselectively into L-**1** (detailed insertion possibilities were discussed in Figure S30). The absence of epimerization in poly(L-**1**) (Figure S4) further confirmed that **Mn-1** was unlikely to have been inserted into the C_4–C_5(O) bond. Note that the formation of Mn(CO) complexes **I1**–**I3** is probably due to the fact that ESI-MS cannot be conducted in completely anhydrous conditions and that Mn complexes undergo carbonylation in an aqueous solution.[30]

Scheme 2. Proposed Mechanism of Mn/Zn-mediated controlled ring-opening polymerization of *O*-carboxyanhydrides (OCAs)

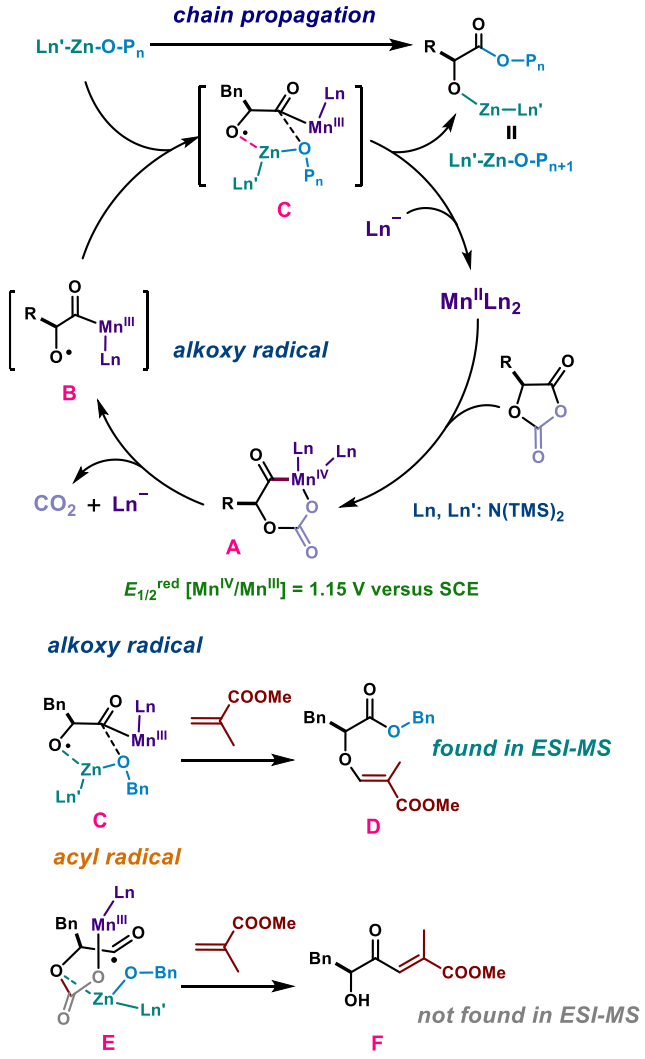

Decarboxylation of **A** furnishes a radical species (Scheme 2), as confirmed by our finding that the addition of the radical scavenger 2,2-di(4-*tert*-octylphenyl)-1-picrylhydrazyl (DPPH) markedly inhibited the ROP (Table S3, entry 10), in a manner similar to that observed for single-electron-transfer reactions involving Ni/Ir photocatalysts.[11b,13,31] On the basis of our prior studies[11b] and literature reports,[31-32] we reasoned that Mn-mediated decarboxylation could result in either alkoxy radical **B** or acyl radical **E** (Scheme 2; the acyl and alkoxy radical pathways are compared in Figure S30a). Since these putative intermediates would be highly reactive, we added an alkene with an electron-withdrawing group to a reaction mixture

containing L-**1**/**Mn-1**/**Zn-1**/BnOH (1/1/1/1) at −15 °C with the goal of capturing and identifying the radical species.[33] Monitoring the reaction by ESI-MS revealed the formation of **D**, instead of **F**, indicating that decarboxylation generates an alkoxy radical (Scheme 2; see Figure 3b for ESI-MS results). The alkoxy radical is then rapidly intercepted by the Zn complex to generate a reactive Zn-alkoxide terminus, thereby enabling regeneration of the Mn^{II} catalyst (Scheme 2).

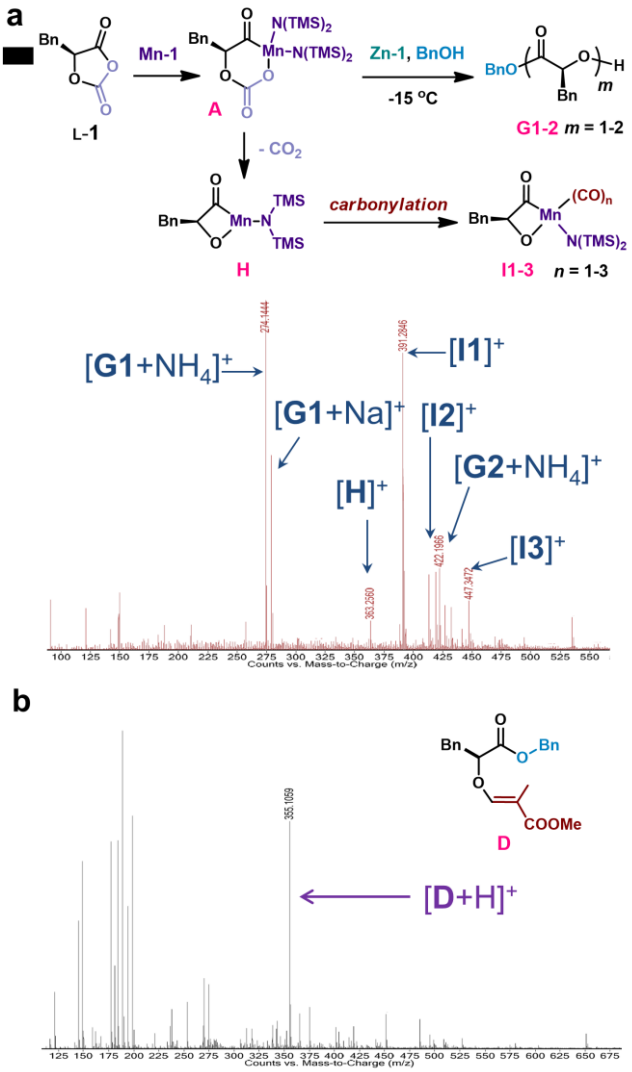

Figure 3. Electrospray ionization mass spectrometry (ESI-MS) of (a) the reaction of [L-**1**]/[**Zn-1**]/[**Mn-1**]/[BnOH] (1/1/1/1) at −15 °C, and (b) the reaction of [L-**1**]/[**Zn-1**]/[**Mn-1**]/[BnOH]/[alkene] at −15 °C, in support of the pathway shown in Scheme 2. Detailed peak assignments and mechanism pathway discussions are provided in Figures S29-30.

The alkoxy radical is reportedly difficult to detect by electron paramagnetic resonance spectroscopy (EPR).[34] While the paramagnetic **Mn-1** showed signals in the X-band continuous wave EPR spectrum at 77 K (Figure S31a), no obvious peaks were found in the mixture of either L-**1**/**Mn-1** (1/1) or L-**1**/**Mn-1**/**Zn-1**/BnOH (1/1/1/1, Figure S31b-c), likely due to the short-lived alkoxy radical species. To test the existence of such radical species, the radical scavenger DPPH—that shows hyperfine splitting peaks in the EPR spectrum at room temperature—was added to the reaction mixture of and L-**1**/**Mn-1**(1/1); the intensity of the splitting peaks from DPPH significantly decreased, suggesting that the alkoxy radical reacted with unpaired-electron-containing DPPH (Figure 4). Furthermore, the addition of DPPH to the mixture L-**1**/**Mn-1**/**Zn-1**/BnOH (1/1/1/1) led to substantially decreased peaks in EPR, suggesting the increased production of alkoxy radical species in the Zn/Mn-mediated ring-opening process (Figure 4).

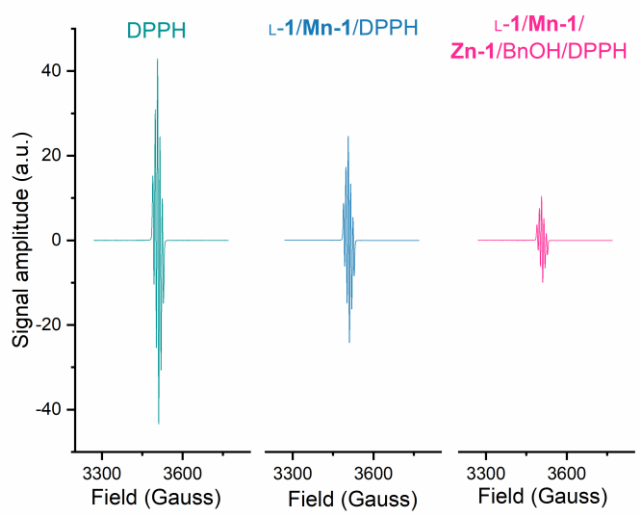

Figure 4. Electron paramagnetic resonance (EPR) study of using DPPH (2,2-di(4-*tert*-octylphenyl)-1-picrylhydrazyl) to quench radical species in Mn/Zn-mediated ring-opening reaction of L-**1** (298 K). Reaction condition: [DPPH] = [**Mn-1**] = [**Zn-1**] = [BnOH] = [L-**1**] = 9.05 mM in toluene at -15 °C for all reactions.

Stereoselective polymerization of racemic OCAs. We then determined whether the Mn/Zn catalytic system could be adapted for stereoselective ROP of racemic OCAs. We previously reported that a Zn complex with a tridentate ligand mediates isoselective photoredox ROP[5b,12b] and electrochemical ROP[12a] to afford stereoblock (*sb*) copolymers. In this study, we found that a similar complex, **Zn-2**, which has a methyl lactate leaving group, also mediated isoselective ROP (Scheme 3; details regarding the screening of Zn and Hf complexes are presented in Table S9). The combination of **Zn-2** and **Mn-1** ([L-**1**]/[D-**1**]/[**Zn-2**]/[**Mn-1**] = 200/200/1/1) at −15 °C produced stereoblock copolymer poly(*sb*-**1**) with a M_n of 56.2 kDa (which is close to the calculated MW of 59.3 kDa), a narrow $Đ$ (1.03), and a high probability of meso dyad formation (P_m, 0.95; Table S9, entry 5; Figure S32). ROP of *rac*-**1** at the same [**1**]/[Zn] ratio without **Mn-1** ([L-**1**]/[D-**1**]/[**Zn-2**] = 200/200/1) showed incomplete monomer conversion (81.3% at 48 hours) with a P_m value of 0.96 (Table S9, entry 7). The use of **Mn-1** likely improved the polymerization kinetics but did not affect the stereochemistry preference. The ^{13}C NMR analysis of the α-methine peaks showed that the ratio of tetrad peaks *mmr* / *rmm* / *mrm* was about 1/1/1 (Figure S32b). Additionally, because the polymerization of either enantiomer at the same [**1**]/[Zn] ratio was identical and more rapid than the ROP of *rac*-**1** (at a [**1**]/[Zn] ratio of 400, the polymerization rate constant of L-**1** was 74.1-times higher than that of *rac*-**1**, Figure S32c), it was unlikely that enantiomorphic-site-control mechanism dominated in this isoselective

Scheme 3. Screen of various Zn and Hf complexes for isoselective ROP of L-1 in the presence of Mn-1 [a]

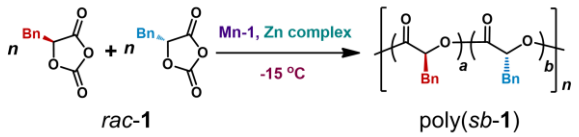

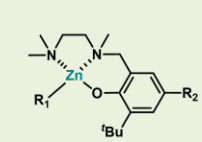

	R_1	R_2	P_m
Zn-2	OCH(Me)CO_2Me	^{t}Bu	0.95
Zn-3	N($SiMe_3$)$_2$	^{t}Bu	0.90
Zn-4	Et	^{t}Bu	conversion < 5%
Zn-5	OCH(Me)CO_2Me	OMe	0.86
Zn-6	OCH(Me)CO_2Me	NO_2	conversion: 56 %
Zn-7	OCH(Me)CO_2Me	F	0.93

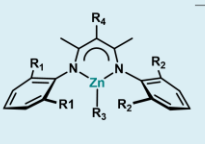

	R_1	R_2	R_3	R_4	P_m
Zn-8	^{i}Pr	^{i}Pr	N($SiMe_3$)$_2$	H	0.73
Zn-9	^{i}Pr	^{i}Pr	OCH(Me)CO_2Me	H	conversion: 31 %
Zn-10	Et	Et	N($SiMe_3$)$_2$	H	0.68
Zn-11	Et	Et	OCH(Me)CO_2Me	H	0.83
Zn-12	Et	^{i}Pr	N($SiMe_3$)$_2$	H	0.75
Zn-13	Et	^{i}Pr	OCH(Me)CO_2Me	H	0.84
Zn-14	Et	Et	OCH(Me)CO_2Me	CN	0.77

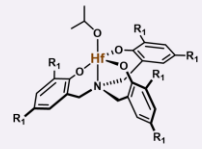

	R_1	P_m
Hf-1	^{t}Bu	conversion: 23 %
Hf-2	Me	conversion: 24 %

[a] Reaction condition: [L-**1**]/[D-**1**]/[**Mn-1**]/[Zn or Hf] = 100/100/1/1, −15 °C in a glove box. P_m, maximum probability of meso dyad formation, determined by ^{13}C NMR spectroscopy. Monomer conversion was determined from the intensity of the Fourier transform infrared peak at 1805 cm^{-1}, which corresponds to the anhydride group in **1**. Polymer MWs and *Đ*s are presented in Table S9.

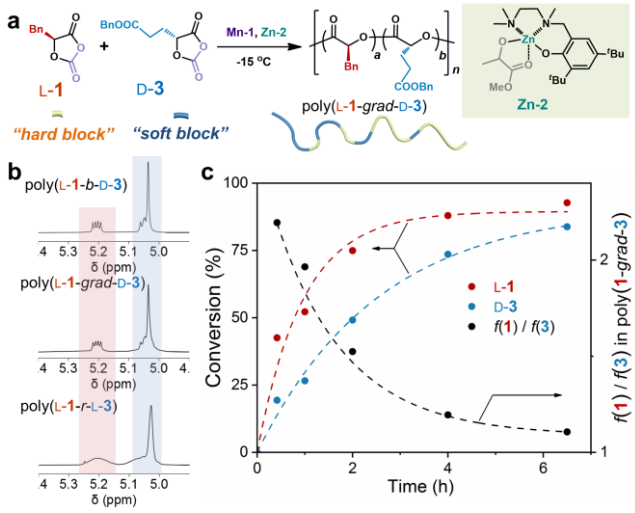

Figure 5. Synthesis and characterization of a gradient copolymer. (a) One-pot **Mn-1**/**Zn-2**-catalyzed ring-opening polymerization of L-1 and D-3 to synthesize poly(L-**1**-*grad*-D-**3**). (b) ^{1}H NMR spectra of highly isotactic poly(L-**1**-*grad*-D-**3**), block copolymer poly(L-**1**-*b*-D-**3**), and random copolymer poly(L-**1**-*r*-L-**3**). Peaks corresponding to the α-methine protons of **1** (~5.2 ppm) and **3** (~5.0 ppm) are highlighted in red and blue, respectively. (c) Kinetics of L-**1** and D-**3** copolymerization to form the gradient copolymer ([L-**1**]/[D-**3**]/[**Mn-1**]/[**Zn-2**] = 200/200/1/1, [L-**1**] = 0.350 M).

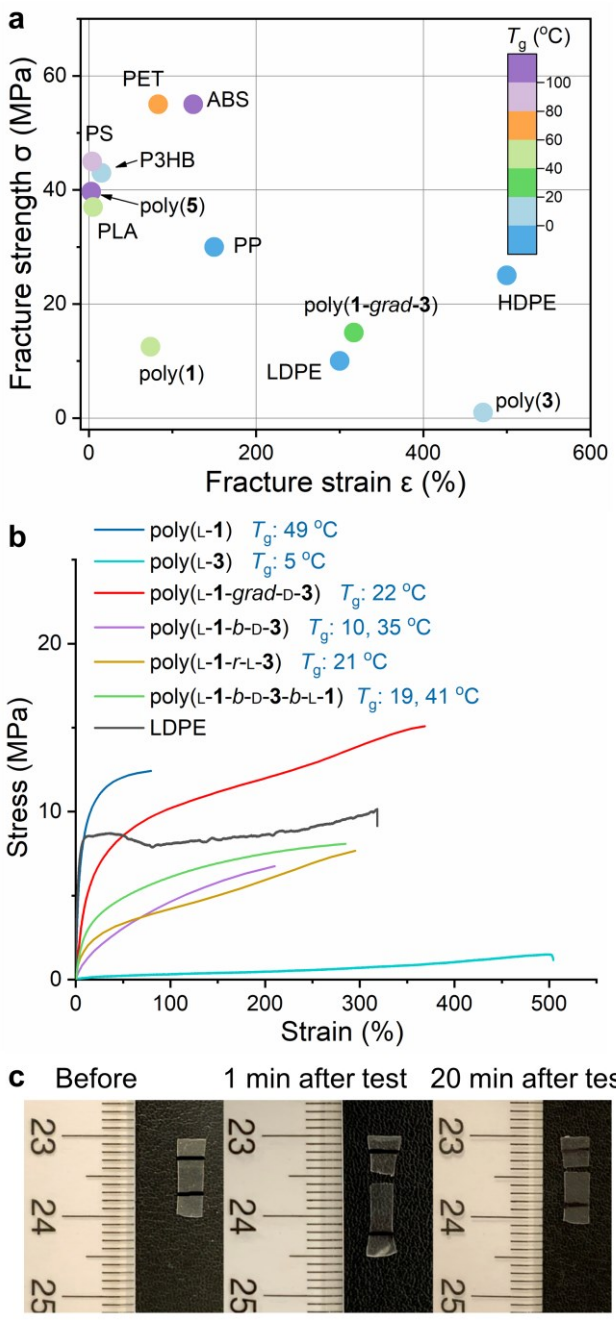

Figure 6. Mechanical study of a ductile and resilient gradient poly(α-hydroxy acid) copolymer. (a) Fracture strengths (σ), fracture strains (ε), and glass-transition temperatures (T_gs) of various poly(α-hydroxy acids), poly(3-hydroxybutyrate) (P3HB), polyethylene terephthalate (PET), comparing with those of commercially available polyolefins, including high-density polyethylene (HDPE), low-density polyethylene (LDPE), polypropylene (PP), polystyrene (PS), and poly(acrylonitrile-butadiene-styrene) (ABS). (b) Representative stress–strain curves for uniaxial extension of various poly(α-hydroxy acids) and LDPE. Polymer MWs and MW weight distributions are provided in Table S11. (c) Rapid shape recovery of poly(L-**1**-*grad*-D-**3**) at room temperature after fracture in the stress–strain test. Also see Movie S1 about the stress-strain test and shape recovery of the gradient copolymer poly(L-**1**-*grad*-D-**3**).

polymerization. Taken together, these results were completely consistent with our previous findings that the use of the same tri-

dentate ligand in the Zn complex led to isoselective ROP via a chain-end-control mechanism.[5b] Furthermore, these two metal complexes also catalyzed isoselective reactions of other racemic OCAs (*rac*-**2**–**5**, Table S10) to afford stereoblock copolymers with P_m values ranging from 0.79 to 0.91 (Figures S33–36).

Our previously reported strategy for the synthesis of gradient (*grad*) copolymers from two OCA co-monomers via photoredox ROP featured the use of an isoselective Zn complex and co-monomers having opposite chiralities and different polymerization rates.[5b] Using a similar strategy for this Mn/Zn-mediated one-pot redox ROP, we found that the combination of **Zn-2** and **Mn-1** at −15 °C mediated gradient copolymerization to generate poly(L-**1**-*grad*-D-**3**) (Figure 5a, Figure S37). We note that at a [**OCA**]/[**Zn-2**] ratio of 200, the polymerization rate constant of L-**1** was 21.7-times higher than that of D-**3** (Figure S37c). ^{1}H NMR spectroscopy confirmed that poly(L-**1**-*grad*-D-**3**) was highly isotactic, as evidenced by the well-defined methine quartet at 5.2 ppm. In comparison, the random (*r*) copolymer poly(L-**1**-*r*-L-**3**) showed a broad peak in this region (Figure 5b). ^{1}H NMR spectroscopic analysis of the copolymerization kinetics showed that L-**1** was converted more rapidly than D-**3**: for instance, at 25 min, conversion of L-**1** was 43%, whereas that of D-**3** was only 19% ([L-**1**]/[D-**3**]/[Zn]/[Mn] = 200/200/1/1; Figure 5c). The L-**1**/D-**3** ratio in the copolymer also decreased markedly with time, from 2.1 at 25 min to 1.2 at 4 h, indicating the formation of a gradient copolymer (Figure 5c). Using the D-**1**/L-**3** pair instead of the L-**1**/D-**3** pair did not affect either the polymerization results or the microstructure of the obtained polymer (Figure S38). Notably, replacing D-**3** with L-**3** resulted in the formation of a random copolymer poly(L-**1**-*r*-L-**3**). This was confirmed by analysis of the polymerization kinetics: the conversions of L-**1** and L-**3** were similar throughout the copolymerization, and the reaction was almost completed within 1 hour (Figure S40c). These results suggested that the use of co-monomers with the same chirality is more likely to result in stereoerrors—and thereby the formation of random copolymers—than the use of co-monomers with different chirality. Using this one-pot copolymerization strategy for monomers with opposite chiralities, we were able to prepare other gradient copolymers from various OCA enantiomers, including poly(L-**1**-*grad*-D-**2**) (Figure S41) and poly(D-**2**-*grad*-L-**3**) (Figure S42).

Resilient gradient copolymer with improved strength and ductility. Copolymers comprising elastic (soft) and glassy (hard) blocks usually exhibit characteristics of thermoplastic elastomers.[35] Our studies of the T_g values and stress–strain characteristics of the homopolymers (Figure 6a), which were enabled by our scalable Mn/Zn-catalyzed reactions to prepare high-MW polyesters, indicated that poly(**1**) could be used as hard blocks and poly(**3**) could be used as soft blocks (Table 3, entries 1 and 3). High-MW poly(L-**1**) (M_n = 170.9 kDa) exhibited a fracture strength (σ) of 12.5 MPa and a fracture strain (ε) of 73.6%, showing improved toughness than low-MW poly(L-**1**) (Table 3, entries 1 versus 2); whereas poly(L-**3**) exhibited elastomeric behavior with no obvious yield point, having an extremely high ε (472%) and a relatively low σ (0.97 MPa; Figure 6b).

Although sequential addition of co-monomers is a well-established method for preparing block copolymers with tailored thermal and mechanical properties, recent studies have suggested that stereosequenced copolymers may exhibit unprecedented thermal or mechanical properties.[5a] Indeed, we discovered in this study that the stereosequences of copolymers did in fact affect their thermal and mechanical properties (Figure 6b). The gradient copolymer poly(L-**1**-*grad*-D-**3**) was stronger and more ductile than the block copolymer poly(L-**1**-*b*-D-**3**) and the random copolymer poly(L-**1**-*r*-L-**3**). Specifically, the σ of poly(L-**1**-*grad*-D-**3**) (14.8 MPa) was 2.46, 2.14, 1.97, and 1.18 times the respective values for poly(L-**1**-*b*-D-**3**), poly(L-**1**-*r*-L-**3**), poly(L-**1**-*b*-D-**3**-*b*-L-**1**), and poly(L-**1**); and the ε value (317.5%) was 1.36, 1.08, 1.21, and 4.31 times the respective values for poly(L-**1**-*b*-D-**3**), poly(L-**1**-*r*-L-**3**), and poly(L-**1**), respectively (Table 3, entries 4-7, and 1). The overall toughness value for poly(L-**1**-*grad*-D-**3**) was dramatically higher than the values for the two corresponding homopolymers (by factors of 4.84 and 12.3, respectively) and the values for poly(L-**1**-*b*-D-**3**), poly(L-**1**-*b*-D-**3**-*b*-L-**1**), and poly(L-**1**-*r*-L-**3**) (by factors of 3.92, 2.55, and 2.86, respectively). Such mechanical properties of poly(L-**1**-*grad*-D-**3**) are comparable to commercially available non-degradable low-density polyethylene (LDPE) (Figure 6b; Table 3, entries 4 versus 8). Notably, varying the ratio between L-**1** and D-**3** in gradient copolymers did not improve the strength and toughness of the copolymers (Table S11, Figure S46b). Additionally, poly(L-**1**-*grad*-D-**3**) only had one T_g (22 °C), which was similar to the T_g of the random copolymer poly(L-**1**-*r*-L-**3**) (21 °C); whereas the block copolymer poly(L-**1**-*b*-D-**3**) had two T_g values (9 and 30 °C, Figure S49). The stereocomplex (*sc*) of poly(L-**1**-*grad*-D-**3**) and poly(D-**1**-*grad*-L-**3**) had an ε value of up to 392 %, but stereocomplex formation did not markedly affect the T_g and σ values, presumably because of the low crystallinity of poly(**3**) (Table S11, Figure S46b and S49).

Additionally, poly(L-**1**-*grad*-D-**3**) showed resilience: a fractured sample of this polymer after the stress–strain test recovered its shape within 20 min at room temperature with a residual strain of 13.2% (Figure 6c; also see Movie S1 about the polymer shape recovery after relieving the stress). The residual strain could be easily recovered when the polymer was kept at 40 °C for 1 h (above its T_g [22 °C]); the strain recovery ratio was 0.948 (Table 3, entry 4). Introduction of a highly elastic poly(**3**) block into gradient or block copolymers provided copolymers with decent strain recovery ratios (ranging from 0.46 to 0.95); whereas poly(L-**1**) and LDPE did not show any pronounced shape memory properties (Table 3, entries 1 and 8; Figures S50 and S51).

CONCLUSIONS

The mainstream adoption of polyesters in plastics engineering has been stymied by a lack of general methods for preparing functionalized polyesters at scale and the consequent lack of information about their structure–property relationships, information that is necessary for the development of degradable alternatives to unsustainable polyolefins. Herein, we describe the mechanism-inspired identification of a redox-active Mn complex that can be used for scalable synthesis of stereoregular polyesters with pendant functional groups and for elucidation of a catalytic reaction pathway that is distinguishable from the conventional coordination-insertion ring-opening pathway. This synthetic method is operationally simple and does not require external energy triggers compared to our previously reported methods. The method can be

used to prepare homopolymers, block copolymers, stereoblock copolymers, and gradient copolymers; and, in particular, it allows us to prepare a gradient copolymer that is tougher, more ductile, and more resilient than the corresponding block copolymers and homopolymers, and outperforms commodity polyolefins such as LDPE in terms of shape recovery resilience (Figure 6c versus Figures S47j and S51i; Table 3). Studies aimed at elucidating how

Table 3. Thermal and mechanical properties of various poly(α-hydroxy acids), compared with LDPE [a]

Entry	Polymer	M_n (kDa) [b]	Đ [b]	T_g / T_m (°C) [c]	E_y (MPa) [d]	σ (MPa) [d]	ε (%) [d]	Strain recovery ratio [e]
1	poly(L-**1**)	170.9	1.09	49 / -	391 ± 46	12.5 ± 0.8	73.6 ± 11.6	0.0058
2	poly(L-**1**)	48.2	1.04	44/ -	87 ± 18	4.9 ± 0.3	53.7 ± 1.7	0
3	poly(L-**3**)	133.8	1.02	5 / 136	1.05 ± 0.06	0.97 ± 0.15	471.6 ± 51.3	0.940
4	poly(L-**1**-*grad*-D-**3**)	65.9	1.02	22 / -	85 ± 34	14.8 ± 0.4	317.5 ± 38.6	0.948
5	poly(L-**1**-*b*-D-**3**)	54.0	1.02	10, 35 / -	8.2 ± 0.7	6.0 ± 0.6	233.5 ± 42.1	0.936
6	poly(L-**1**-*r*-L-**3**)	67.4	1.05	21 / -	40 ± 24	6.9 ± 0.8	294.9 ± 43.2	0.946
7	poly(L-**1**-*b*-D-**3**-*b*-L-**1**)	64.0	1.07	19, 41 / -	44.3 ± 25.7	7.5 ± 0.9	262.6 ± 22.3	0.950
8	LDPE	-	-	-	160 ± 55	9.95 ± 0.2	311.6 ± 10.9	0.012

[a] Abbreviations: M_n, number-average molecular weight; *Đ*, molecular weight distribution; T_g, glass transition temperature; T_m, melting temperature; E_y, Young's modulus; σ, fracture stress; ε, fracture strain; *sb*, stereoblock; *sc*, stereocomplex; *grad*, gradient; *b*, block; *r*, random; LDPE, low-density polyethylene. For all mechanical tests, n = 4-5, and data are presented as mean ± standard deviation. [b] Determined by gel-permeation chromatography. [c] Determined by differential scanning calorimetry (Figures S48-S49). [d] Determined by stress-strain tests (Figure 6b). [e] The equation for strain recovery ratio is described in Section 2.11 (results in Figures S47 and S51). Other polyesters' thermal and mechanical tests results are presented in Figures S46-S51 and Table S11-13.

stereosequence influences mechanical properties and at expanding the scope of stereosequences to include syndiotactic blocks are underway. We anticipate that the findings described herein will accelerate the discovery of new polyester materials by allowing for control of polymer stereosequences. Use of the resulting degradable polyester elastomers for packaging, fiber, and biomedical applications can be foreseen.

ASSOCIATED CONTENT

Supporting Information.

The Supporting Information is available free of charge on the ACS Publications website.

- Detailed experimental procedures; monomers and catalysts synthesis; catalyst screening and reaction optimization; polymerization kinetics and characterization (ESI-MS and MALDI spectroscopy, NMR spectroscopy; GPC); mechanistic considerations and characterization (ESI-MS spectroscopy, CV, infrared spectroscopy, EPR spectroscopy) and reaction pathways discussion; thermal and mechanical tests of polymers (DSC, tensile tests, shape-memory tests)
- EPR raw data
- The movie of the tensile test and shape recovery of the gradient copolymer

AUTHOR INFORMATION

Corresponding Author

* rtong@vt.edu

Funding Sources

This work was supported by start-up funding from Virginia Tech, ACS-Petroleum Research Foundation (57926-DNI-7), and the National Science Foundation (CHE-1807911).

Notes

The authors declare no competing financial interest.

ACKNOWLEDGMENT

We thank Dr. N. Murthy Shanaiah (Department of Chemistry, Virginia Tech) for NMR experiments, Mehdi Ashraf-Khorassani (Department of Chemistry, Virginia Tech) for ESI-MS studies, Dr. Ling Li (Department of Mechanical Engineering, Virginia Tech) and Dr. Thomas Staley (Department of Materials Science and Engineering, Virginia Tech) for mechanical testing, Dr. Jeffrey Parks (Department of Civil & Environmental Engineering, Virginia Tech) for inductively coupled plasma mass spectrometry measurements, Dr. Toby Woods (Department of Chemistry, University of Illinois) for EPR experiments, and Dr. Webster Santos and Dr. John Matson (Department of Chemistry, Virginia Tech) for providing anhydrous solvents.

REFERENCES

(1) Rochman, C. M.; Browne, M. A.; Halpern, B. S.; Hentschel, B. T.; Hoh, E.; Karapanagioti, H. K.; Rios-Mendoza, L. M.; Takada, H.; Teh, S.;

Thompson, R. C. Classify plastic waste as hazardous. *Nature* **2013,** *494,* 169-171.

(2) (a) Zhu, Y.; Romain, C.; Williams, C. K. Sustainable polymers from renewable resources. *Nature* **2016,** *540,* 354-362. (b) Hong, M.; Chen, E. Y. X. Chemically recyclable polymers: a circular economy approach to sustainability. *Green Chem.* **2017,** *19,* 3692-3706. (c) Hillmyer, M. A.; Tolman, W. B. Aliphatic Polyester Block Polymers: Renewable, Degradable, and Sustainable. *Acc. Chem. Res.* **2014,** *47,* 2390-2396. (d) Coates, G. W.; Getzler, Y. D. Y. L. Chemical recycling to monomer for an ideal, circular polymer economy. *Nat. Rev. Mater.* **2020,** *5,* 501-516.

(3) (a) Dechy-Cabaret, O.; Martin-Vaca, B.; Bourissou, D. Controlled ring-opening polymerization of lactide and glycolide. *Chem. Rev.* **2004,** *104,* 6147-6176. (b) Zhu, J.-B.; Watson, E. M.; Tang, J.; Chen, E. Y.-X. A synthetic polymer system with repeatable chemical recyclability. *Science* **2018,** *360,* 398-403.

(4) For representative reviews, see (a) Stanford, M. J.; Dove, A. P. Stereocontrolled ring-opening polymerisation of lactide. *Chem. Soc. Rev.* **2010,** *39,* 486-494. (b) Li, H.; Shakaroun, R. M.; Guillaume, S. M.; Carpentier, J.-F. Recent Advances in Metal-Mediated Stereoselective Ring-Opening Polymerization of Functional Cyclic Esters towards Well-Defined Poly(hydroxy acid)s: From Stereoselectivity to Sequence-Control. *Chem. Eur. J.* **2020,** *26,* 128-138. (c) Thomas, C. M. Stereocontrolled ring-opening polymerization of cyclic esters: synthesis of new polyester microstructures. *Chem. Soc. Rev.* **2010,** *39,* 165-173.

(5) For examples of stereosequence-controlled polyesters, see (a) Tang, X.; Westlie, A. H.; Watson, E. M.; Chen, E. Y.-X. Stereosequenced crystalline polyhydroxyalkanoates from diastereomeric monomer mixtures. *Science* **2019,** *366,* 754-758. (b) Feng, Q.; Yang, L.; Zhong, Y.; Guo, D.; Liu, G.; Xie, L.; Huang, W.; Tong, R. Stereoselective photoredox ring-opening polymerization of *O*-carboxyanhydrides. *Nat. Commun.* **2018,** *9,* 1559.

(6) Worch, J. C.; Prydderch, H.; Jimaja, S.; Bexis, P.; Becker, M. L.; Dove, A. P. Stereochemical enhancement of polymer properties. *Nat. Rev. Chem.* **2019,** *3,* 514-535.

(7) Sangroniz, A.; Zhu, J.-B.; Tang, X.; Etxeberria, A.; Chen, E. Y. X.; Sardon, H. Packaging materials with desired mechanical and barrier properties and full chemical recyclability. *Nat. Commun.* **2019,** *10,* 3559.

(8) (a) Boaen, N. K.; Hillmyer, M. A. Post-polymerization functionalization of polyolefins. *Chem. Soc. Rev.* **2005,** *34,* 267-275. (b) Franssen, N. M. G.; Reek, J. N. H.; de Bruin, B. Synthesis of functional 'polyolefins': state of the art and remaining challenges. *Chem. Soc. Rev.* **2013,** *42,* 5809-5832.

(9) Yu, Y.; Zou, J.; Cheng, C. Synthesis and biomedical applications of functional poly([small alpha]-hydroxyl acid)s. *Polym. Chem.* **2014,** *5,* 5854-5872.

(10) Xu, Y.; Perry, M. R.; Cairns, S. A.; Shaver, M. P. Understanding the ring-opening polymerisation of dioxolanones. *Polym. Chem.* **2019,** *10,* 3048-3054.

(11) (a) du Boullay, O. T.; Marchal, E.; Martin-Vaca, B.; Cossio, F. P.; Bourissou, D. An activated equivalent of lactide toward organocatalytic ring-opening polymerization. *J. Am. Chem. Soc.* **2006,** *128,* 16442-16443. (b) Feng, Q.; Tong, R. Controlled Photoredox Ring-Opening Polymerization of *O*-Carboxyanhydrides. *J. Am. Chem. Soc.* **2017,** *139,* 6177-6182.

(12) (a) Zhong, Y.; Feng, Q.; Wang, X.; Chen, J.; Cai, W.; Tong, R. Functionalized Polyesters via Stereoselective Electrochemical Ring-Opening Polymerization of *O*-Carboxyanhydrides. *ACS Macro Lett.* **2020,** *9,* 1114-1118. (b) Zhong, Y.; Feng, Q.; Wang, X.; Yang, L.; Korovich, A. G.; Madsen, L. A.; Tong, R. Photocatalyst-independent photoredox ring-opening polymerization of *O*-carboxyanhydrides: stereocontrol and mechanism. *Chem. Sci.* **2021,** *12,* 3702-3712.

(13) Zuo, Z. W.; Ahneman, D. T.; Chu, L. L.; Terrett, J. A.; Doyle, A. G.; MacMillan, D. W. C. Merging photoredox with nickel catalysis: Coupling of alpha-carboxyl sp(3)-carbons with aryl halides. *Science* **2014,** *345,* 437-440.

(14) Yu, Y.; Liu, X.; Wang, J. Expansion of Redox Chemistry in Designer Metalloenzymes. *Acc. Chem. Res.* **2019,** *52,* 557-565.

(15) Bullock, R. M. *Catalysis without Precious Metals*; Wiley-VCH Weinheim, Germany, 2010.

(16) (a) Andersen, R. A.; Faegri, K.; Green, J. C.; Haaland, A.; Lappert, M. F.; Leung, W. P.; Rypdal, K. Synthesis of bis[bis(trimethylsilyl)amido]iron(II). Structure and bonding in $M[N(SiMe3)_2]_2$ (M = manganese, iron, cobalt): two-coordinate transition-metal amides. *Inorg. Chem.* **1988,** *27,* 1782-1786. (b) Power, P. P. Stable Two-Coordinate, Open-Shell (d1–d9) Transition Metal Complexes. *Chem. Rev.* **2012,** *112,* 3482-3507. (c) Hu, A.; Guo, J.-J.; Pan, H.; Zuo, Z. Selective functionalization of methane, ethane, and higher alkanes by cerium photocatalysis. *Science* **2018,** *361,* 668-672.

(17) Walsh, C. T. Biologically generated carbon dioxide: nature's versatile chemical strategies for carboxy lyases. *Nat. Prod. Rep.* **2020,** *37,* 100-135.

(18) Li, M.; Zhang, S.; Zhang, X.; Wang, Y.; Chen, J.; Tao, Y.; Wang, X. Unimolecular Anion-Binding Catalysts for Selective Ring-Opening Polymerization of *O*-carboxyanhydrides. *Angew. Chem. Int. Ed.* **2021,** *60,* 6003-6012.

(19) Webster, O. W. Living Polymerization Methods. *Science* **1991,** *251,* 887-893.

(20) Buchard, A.; Carbery, D. R.; Davidson, M. G.; Ivanova, P. K.; Jeffery, B. J.; Kociok-Köhn, G. I.; Lowe, J. P. Preparation of Stereoregular Isotactic Poly(mandelic acid) through Organocatalytic Ring-Opening Polymerization of a Cyclic *O*-Carboxyanhydride. *Angew. Chem. Int. Ed.* **2014,** *53,* 13858-13861.

(21) Yang, R.; Xu, G.; Lv, C.; Dong, B.; Zhou, L.; Wang, Q. $Zn(HMDS)_2$ as a Versatile Transesterification Catalyst for Polyesters Synthesis and Degradation toward a Circular Materials Economy Approach. *ACS Sustain. Chem. Eng.* **2020,** *8,* 18347-18353.

(22) Planer, S.; Jana, A.; Grela, K. Ethyl Lactate: A Green Solvent for Olefin Metathesis. *ChemSusChem* **2019,** *12,* 4655-4661.

(23) Koshikari, Y.; Sakakura, A.; Ishihara, K. N,N-Diarylammonium Pyrosulfate as a Highly Effective Reverse Micelle-Type Catalyst for Hydrolysis of Esters. *Org. Lett.* **2012,** *14,* 3194-3197.

(24) (a) Leibfarth, F. A.; Moreno, N.; Hawker, A. P.; Shand, J. D. Transforming polylactide into value-added materials. *J. Polym. Sci. A Polym. Chem.* **2012,** *50,* 4814-4822. (b) Codari, F.; Lazzari, S.; Soos, M.; Storti, G.; Morbidelli, M.; Moscatelli, D. Kinetics of the hydrolytic degradation of poly(lactic acid). *Polym. Degrad. Stab.* **2012,** *97,* 2460-2466.

(25) Fukushima, K.; Coulembier, O.; Lecuyer, J. M.; Almegren, H. A.; Alabdulrahman, A. M.; Alsewailem, F. D.; Mcneil, M. A.; Dubois, P.; Waymouth, R. M.; Horn, H. W.et al. Organocatalytic depolymerization of poly(ethylene terephthalate). *J. Polym. Sci. A Polym. Chem.* **2011,** *49,* 1273-1281.

(26) Nishida, H.; Mori, T.; Hoshihara, S.; Fan, Y.; Shirai, Y.; Endo, T. Effect of tin on poly(L-lactic acid) pyrolysis. *Polym. Degrad. Stab.* **2003,** *81,* 515-523.

(27) Zuo, Z.; MacMillan, D. W. C. Decarboxylative Arylation of α-Amino Acids via Photoredox Catalysis: A One-Step Conversion of Biomass to Drug Pharmacophore. *J. Am. Chem. Soc.* **2014,** *136,* 5257-5260.

(28) Reports on Mn-mediated two-electron-transfer redox reactions, see (a) Lynch, M. W.; Hendrickson, D. N.; Fitzgerald, B. J.; Pierpont, C. G. Intramolecular two-electron transfer between manganese(II) and semiquinone ligands. Synthesis and characterization of manganese 3,5-di-tert-butylquinone complexes and their relationship to the photosynthetic water oxidation system. *J. Am. Chem. Soc.* **1984,** *106,* 2041-2049. (b) Romero, I.; Collomb, M.-N.; Deronzier, A.; Llobet, A.; Perret, E.; Pécaut, J.; Le Pape, L.; Latour, J.-M. A Novel Dimanganese(II) Complex with Two Chloride Bridges – A Two-Electron Oxidation System. *Eur. J. Inorg. Chem.* **2001,** *2001,* 69-72.

(29) Steinlechner, C.; Roesel, A. F.; Oberem, E.; Päpcke, A.; Rockstroh, N.; Gloaguen, F.; Lochbrunner, S.; Ludwig, R.; Spannenberg, A.; Junge,

H.et al. Selective Earth-Abundant System for CO_2 Reduction: Comparing Photo- and Electrocatalytic Processes. *ACS Catal.* **2019,** *9,* 2091-2100.

(30) Walsh, J. J.; Neri, G.; Smith, C. L.; Cowan, A. J. Water-Soluble Manganese Complex for Selective Electrocatalytic CO_2 Reduction to CO. *Organometallics* **2019,** *38,* 1224-1229.

(31) Le, C.; MacMillan, D. W. C. Fragment Couplings via CO_2 Extrusion-Recombination: Expansion of a Classic Bond-Forming Strategy via Metallaphotoredox. *J. Am. Chem. Soc.* **2015,** *137,* 11938-11941.

(32) Examples of two plausible radical species, see (a) Dong, S.; Wu, G.; Yuan, X.; Zou, C.; Ye, J. Visible-light photoredox catalyzed hydroacylation of electron-deficient alkenes: carboxylic anhydride as an acyl radical source. *Org. Chem. Front.* **2017,** *4,* 2230-2234. (b) Zhang, J.; Li, Y.; Zhang, F.; Hu, C.; Chen, Y. Generation of Alkoxyl Radicals by Photoredox Catalysis Enables Selective C(sp3)–H Functionalization under Mild Reaction Conditions. *Angew. Chem. Int. Ed.* **2016,** *55,* 1872-1875.

(33) Barthelemy, A.-L.; Tuccio, B.; Magnier, E.; Dagousset, G. Alkoxyl Radicals Generated under Photoredox Catalysis: A Strategy for anti-Markovnikov Alkoxylation Reactions. *Angew. Chem. Int. Ed.* **2018,** *57,* 13790-13794.

(34) Paul, H.; Small, R. D.; Scaiano, J. C. Hydrogen abstraction by tert-butoxy radicals. A laser photolysis and electron spin resonance study. *J. Am. Chem. Soc.* **1978,** *100,* 4520-4527.

(35) Bates, F. S.; Hillmyer, M. A.; Lodge, T. P.; Bates, C. M.; Delaney, K. T.; Fredrickson, G. H. Multiblock Polymers: Panacea or Pandora's Box? *Science* **2012,** *336,* 434-440.

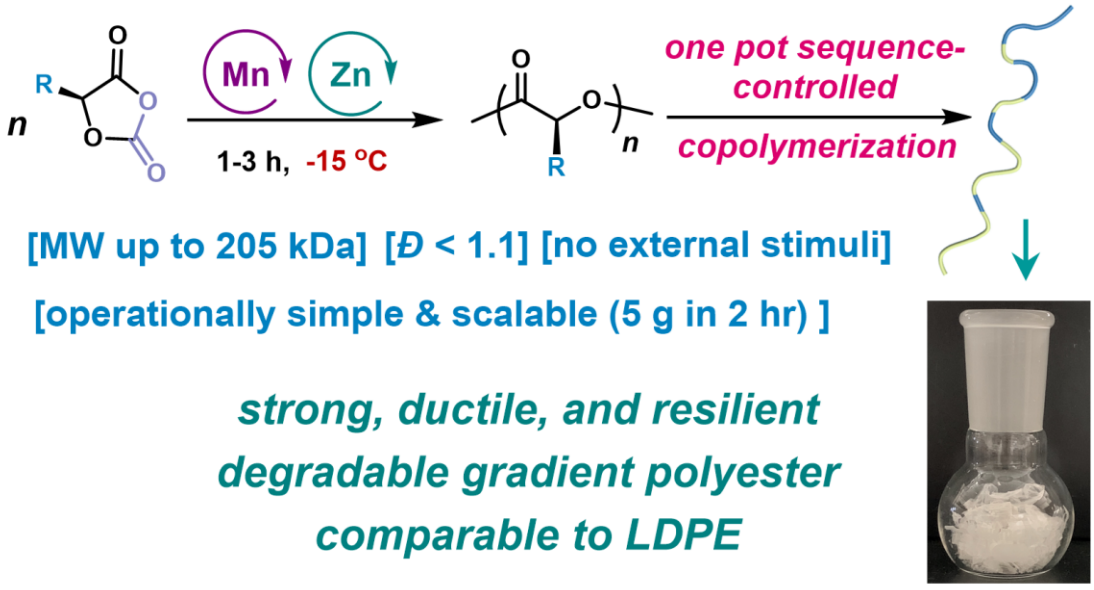
Mn
Zn
1-3 h, -15 °C
one pot sequence-controlled
copolymerization
[MW up to 205 kDa] [Đ < 1.1] [no external stimuli]
[operationally simple & scalable (5 g in 2 hr)]
strong, ductile, and resilient
degradable gradient polyester
comparable to LDPE